Geophysical Journal International

Geophys. J. Int. (2011) doi: 10.1111/j.1365-246X.2011.05239.x

Mantle transition zone thickness beneath Cameroon: evidence for an upper mantle origin for the Cameroon Volcanic Line

Angela Marie Reusch,[1,*] Andrew A. Nyblade,[1] Rigobert Tibi,[2,†] Douglas A. Wiens,[2] Patrick J. Shore,[2] Ateba Bekoa,[3] Charles T. Tabod,[4] and Joseph M. Nnange[5]

[1] *Department of Geosciences, Pennsylvania State University, 441 Deike Bldg, University Park,* PA 16802, *USA. E-mail: nyblade@psu.edu*
[2] *Department of Earth and Planetary Sciences, Washington University, St. Louis,* MO 63130, *USA*
[3] *Branch for Geophysical and Volcanological Research, Institute for Geological and Mining Research, Buea, Cameroon*
[4] *Department of Physics, University of Yaounde I,* PO Box 6052, *Yaounde, Cameroon*
[5] *Institute for Geological and Mining Research,* B.P. 4110, *Yaounde, Cameroon*

Accepted 2011 September 21. Received 2011 September 5; in original form 2011 May 13

SUMMARY

The thickness of the mantle transition zone beneath Cameroon has been mapped using data from the 2005–2007 Cameroon Broadband Seismic Experiment to evaluate models for the origin of the Cameroon Volcanic Line (CVL). Some 2200 receiver functions have been stacked using a 3-D velocity model, revealing P_s conversions from the mantle transition zone discontinuities at depths of ∼410 and 660 km. Results yield a nearly uniform transition zone thickness (251 ± 10 km) that is similar to the global average, implying that any thermal anomalies in the upper mantle beneath the CVL do not extend as deep as the transition zone. This finding, when combined with regional *P* and *S* velocity models of the mantle, supports an explanation attributing the origin of the CVL to upper mantle processes such as an edge flow convection cell in the upper mantle along the northwestern side of the Congo Craton lithosphere.

Key words: Body waves; Dynamics of lithosphere and mantle; Hotspots; Africa.

INTRODUCTION

The ∼1600 km linear Cameroon Volcanic Line (CVL) spans the ocean–continent boundary in West Africa and is comprised of numerous volcanic centres in continental Cameroon and on four islands: Bioko, São Tomé and Príncipe, and Annobon (Fig. 1). The volcanic centres range in age from Eocene to Recent, and are generally alkaline massifs emplaced in a N30° trend, similar to more than 60 Paleocene to early Oligocene anorogenic plutonic complexes (Déruelle *et al.* 1991). The volcanism was initiated as early as 42 Ma, and became widespread along the CVL during the Oligocene (Marzoli *et al.* 1999, 2000). Many of the volcanic centres have had activity in the past one million years (Fitton & Dunlop 1985), with the most recent activity occurring at Mt. Cameroon. The continental portion of the CVL developed within the Pan African Oubanguides or North Equatorial fold belt to the north of the Archean Congo Craton (Fig. 1).

The age pattern of the volcanism is not easily accounted for by a single hotspot beneath a moving plate, as discussed by Morgan (1983), Van Houten (1983), Lee *et al.* (1994) and Burke (2001). Therefore a number of other models for the origin of the CVL have been suggested, such as multiple plumes (Ngako *et al.* 2006), flow from the Afar plume channelled by thinned lithosphere beneath central Africa (Ebinger & Sleep 1998), decompression melting beneath reactivated shear zones (Fairhead 1988; Fairhead & Binks 1991), edge-flow convection (King & Anderson 1995, 1998; King & Ritsema 2000; King 2007), and vertical flow of hot material from the base of the transition zone induced by shear heating below the 660 km discontinuity (Meyers *et al.* 1998). In a recent study, Reusch *et al.* (2010) argued for an edge-flow convection model based upon tomographic images showing a tabular low velocity anomaly (LVA) beneath the CVL extending to at least 300 km depth that is not consistent with much shallower LVAs predicted by plume models. Reusch *et al.* (2010) attributed the LVA to a thermal anomaly of ≥280 K. Because of limitations in model resolution, Reusch *et al.* (2010) could not determine if the LVA extended deeper than ∼300 km. Consequently, they could not fully evaluate the vertical flow model proposed by Meyers *et al.* (1998), nor could they test the edge-flow model by comparing the depth of the LVA against the depth predicted by the distance between the CVL and the Congo Craton.

In this study, we investigate the depth extent of the LVA beneath the CVL by mapping the topography of the 410 and 660 km discontinuities using receiver-function stacks from teleseismic earthquakes recorded by the Cameroon Broadband Seismic Experiment (Tibi *et al.* 2005). The mantle transition zone is bounded by discontinuities at the globally average depths of 410 and 660 km that

*Now at: IRIS PASSCAL Instrument Center, New Mexico Tech, 801 Leroy Pl, Socorro, NM 87801, USA.
†Now at: P.C. Rizzo Associates, Inc., Pittsburgh, PA 15235, USA.

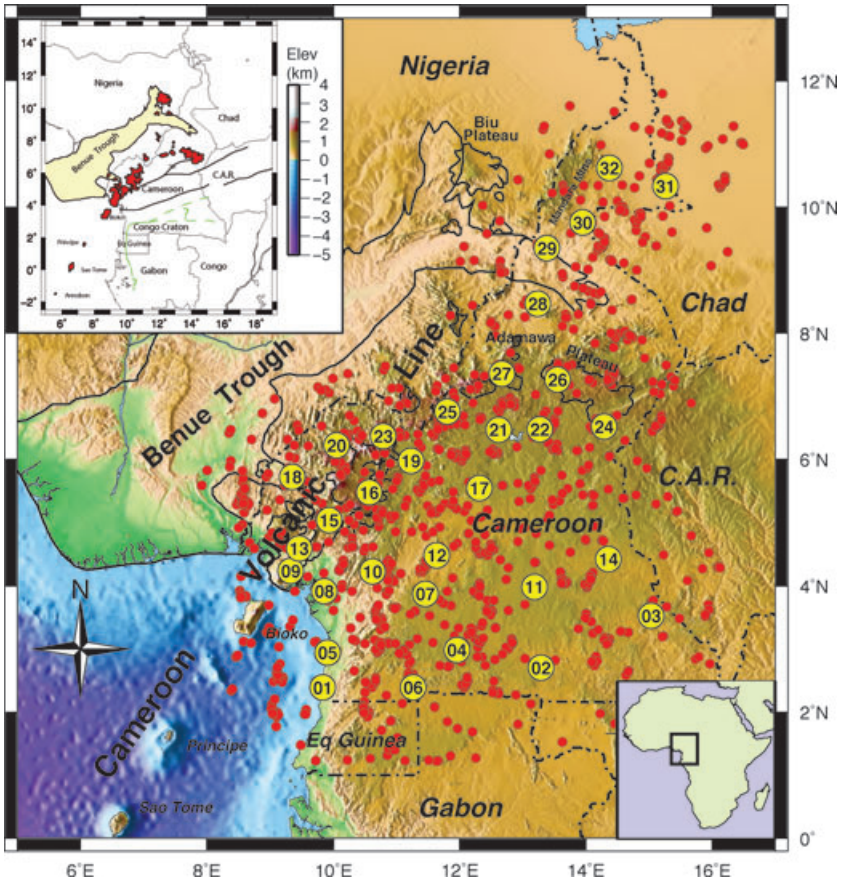

Figure 1. Topographic map showing seismic station locations (yellow circles) for this study. Political boundaries are marked by the dot-dash line (C.A.R., Central African Republic). The inset map at the bottom right-hand corner shows the location of the larger map on the continent of Africa and the inset map at the top left-hand corner shows the location of the major volcanic centres in red, the Benue Trough in yellow and the northwestern boundary of the Congo Craton with a green line. The ray-theoretical P_s conversion points at 410 km depth are indicated with red dots.

are generally interpreted as mineral phase transformations in olivine (Bina & Helffrich 1994). Because the slopes of the phase transitions on a pressure–temperature plot (Clapeyron slopes), are opposite in sign for the 410 and 660 km discontinuities, the transition zone thickness (TZT), defined as the thickness of the region between the discontinuities, can provide information about the thermal structure of the upper mantle. So, for example, a thinner-than-average TZT indicates a warm thermal anomaly, whereas a thicker-than-average TZT would be a cooler thermal anomaly. By mapping the topography of the 410 and 660 km discontinuities and determining the thickness between them, we can address whether or not the LVA imaged using body-wave tomography (Reusch *et al.* 2010) is a deep-seated thermal anomaly extending well into the mantle transition zone, as predicted by the Meyers *et al.* (1998) model, or a shallower anomaly more consistent with the edge-flow model.

MANTLE TRANSITION ZONE *P* WAVE RECEIVER FUNCTIONS

The data used in this study were recorded between 2005 January and 2007 February by the Cameroon Broadband Seismic Experiment, which consisted of 32 portable broad-band seismometers installed across Cameroon, West Africa (Fig. 1). Data from earthquakes with $m_b \geq 5.0$, located at epicentral distances of between 30° and 90° and distributed over a wide range of back azimuths were used for this study. The time domain iterative deconvolution method of Ligorría & Ammon (1999), applied to seismograms rotated into vertical, radial and transverse components, is used to generate the receiver functions. The ray-theoretical P_s conversion points at a depth of 410 km for the 2210 station-event pairs used are shown in Fig. 1 to demonstrate the spatial coverage of the data set.

Following the Owens *et al.* (2000) methodology, a geographical binning technique that included a 3-D velocity model of the upper mantle was used to stack the radial receiver functions. The 3-D velocity model was taken from Reusch *et al.* (2010), where *P* and *S* relative traveltime residuals were used to invert for upper mantle velocity variations. Crustal structure in the 3-D model was taken from Tokam *et al.* (2010). Using the 3-D model, the traveltime and piercing point for every P_s conversion were calculated from 0 to 800 km depth for each station-event pair in 10 km intervals. The traveltime for a P_s conversion at a specified depth was used to extract the amplitude from each receiver function. Then, for that depth, all of the amplitude measurements falling within a circular region (bin) were stacked. Permutations in the stacking procedure that were tried included changing the diameter of the bin, altering the minimum number of measurements in each bin, varying the minimum number of stations represented in each bin, and performing the stacking using the 1-D IASP91 model from Kennett & Engdahl (1991).

We found that the optimal stacking parameters included a minimum of 30 receiver functions per bin from at least four stations,

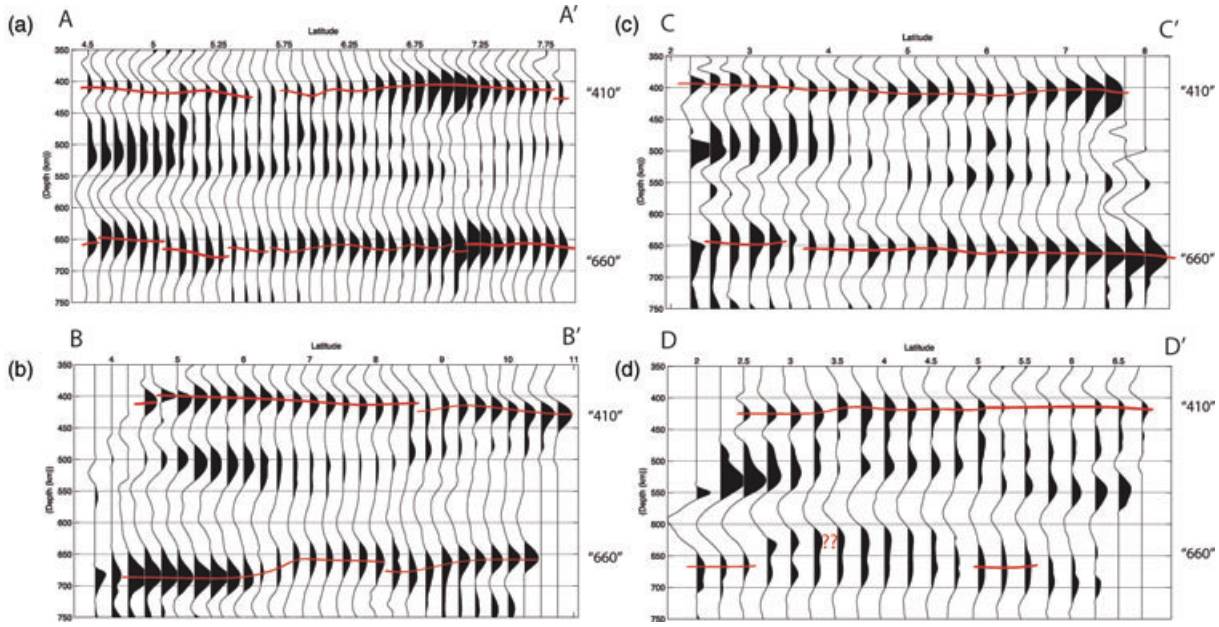

Figure 2. Profiles of receiver function stacks showing P_s conversions in the 350–750 km depth interval. The locations of the profiles are given in Fig. 3. The red lines show the P_s conversions from the 410 to 660 km discontinuities.

a bin radius of 1.0°, a bin increment of 0.25° and a Gaussian filter width of 0.5 for computing the receiver functions. The addition of P_s conversions from *PP* waves resulted in less coherent stacks with either elongated or complex arrivals, and therefore they were not used.

Owens *et al.* (2000) found that for their method of stacking receiver functions with a 3-D velocity model, the precision of the depth estimate of the discontinuities is on the order of ±3 km. However, because of uncertainties in crustal thickness (Tokam *et al.* 2010), and upper mantle velocities (Reusch *et al.* 2010), we estimate the uncertainties in the inferred discontinuity depths to be in the order of ±5 km.

Several receiver function profiles are shown in Fig. 2, illustrating the quality of the receiver function stacks. On profiles A–A′, B–B′ and C–C′ clear P_s arrivals from the 410 and 660 km discontinuities can be seen. Although a slight apparent deepening of both discontinuities is seen with increasing latitude, likely due to lateral velocity variations within the region above the transition zone, overall the TZT remains unchanged across the profiles. Even though the stacked P_s arrivals are adjusted for lateral heterogeneity in upper mantle structure using a 3-D velocity model, the depths of the discontinuities could remain biased from the true depths because structure in the velocity model is not fully resolved. Therefore, changes in the TZT provide a more robust indication of a thermal perturbation at transition zone depths than do the absolute depths of the 410–660 km discontinuities. In addition, all four profiles show coherent arrivals in some locations around depths of 500 ± 20 km. These arrivals possibly correspond to the 520 km discontinuity, but they are not continuous across the profiles or as clear as the P_s arrivals from the 410 or 660 km discontinuities. Therefore, we do not interpret them.

A map showing the TZT for the study area is displayed in Fig. 3. In spite of small variations in the topography of the 410 and 660 km discontinuities seen in the receiver function stacks, the overall TZT remains fairly consistent across the study area, with an average of 251 ± 10 km. For the majority of the study area, there is a variability of about ±10 km in the thickness between stacked receiver functions, but this variability falls within the uncertainty of the individual TZT estimates.

An unusual area with respect to the rest of the study area is identified in Fig. 3 by the region coloured in red, located in the southwestern part of Cameroon encompassing part of the northern edge of the Congo Craton and the mobile belt. This region is characterized by two P_s arrivals in the 600–700 km depth interval (see phases noted with question marks on profile D–D′ in Fig. 2). If the deeper arrival is picked as the '660', then a TZT consistent with the rest of the study region is obtained (i.e. ∼240–250 km). The nature of the coherent arrival at ∼620 km depth is not clear. One possibility is that the arrival originates from scattering at that depth caused by small-scale structure. Alternatively, the arrival could constitute a multiple phase from a deeper and a shallower interface. Because it is not clear why there is a coherent arrival at ∼620 km depth, we opt not to include the results for this region in the average TZT we report. Perhaps related to the same geographical region is the appearance of negative arrivals at a depth of ∼550–600 km at the southerly end of lines A–A′, C–C′ and D–D′. The southern ends of these three lines all fall close to or inside the red-marked region in Fig. 3, and perhaps complex structure in this region at these depths could be contributing to the strong amplitude negative arrivals, as well as the double P_s arrivals between 600 and 700 km depth.

DISCUSSION AND CONCLUSIONS

The main finding of this study is that there is no obvious difference in the TZT beneath the CVL compared to the regions adjacent to it. The average TZT of 251 ± 10 km is comparable to global estimates of average TZT thickness, which range from 242 to 260 km (Flanagan & Shearer 1998; Chevrot *et al.* 1999; Lawrence & Shearer 2006); Courtier *et al.* 2007. Thus, there is little, if any, evidence for a thermal anomaly within the transition zone.

As discussed in the introduction, Reusch *et al.* (2010) found a tabular velocity anomaly under the CVL, which they attributed to a temperature anomaly of ≥280 K, extending to at least 300 km

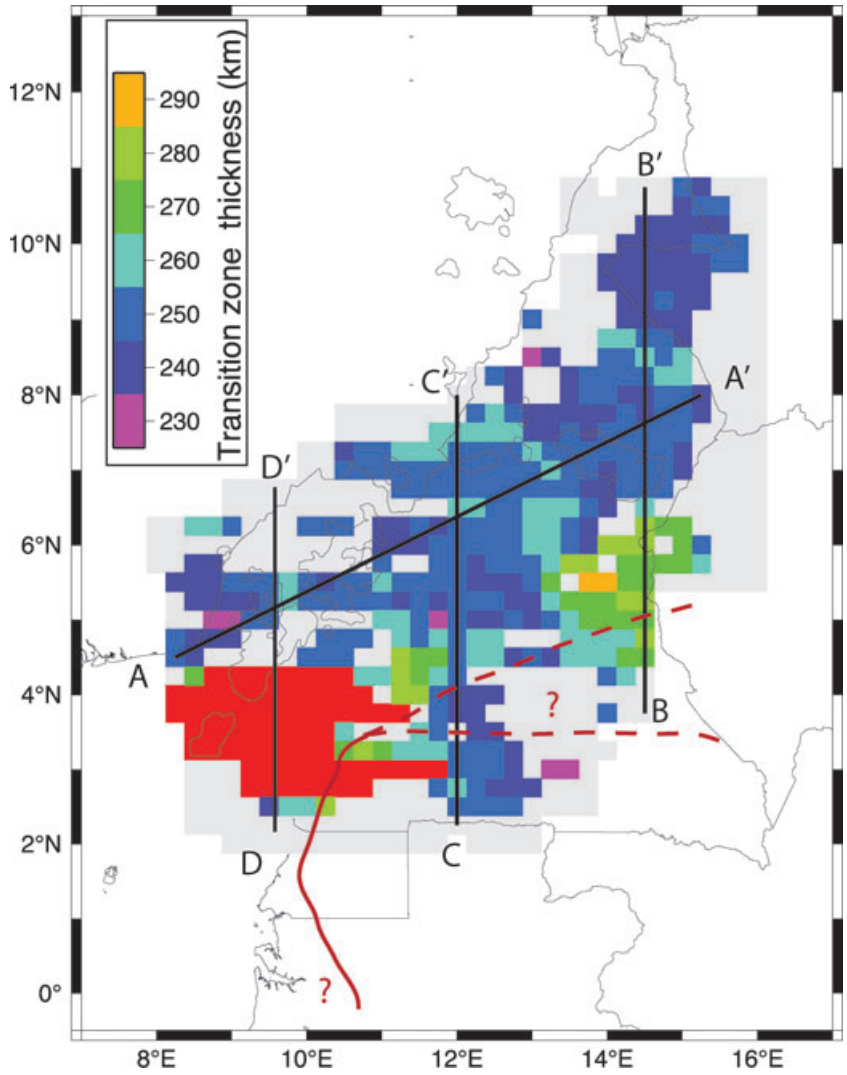

Figure 3. Map showing transition zone thickness. Each coloured square represents a 1° radius bin along a grid with 0.25° spacing. The light grey squares indicate areas where the transition zone thickness could not be mapped and the red squares show locations where there is uncertainty in picking the 660 because of a strong arrival at ∼620 km depth. The CVL volcanics are outlined in black. The solid red line shows the northern boundary of the Congo craton, and the dashed red lines show possible locations of the boundary in the eastern part of the study area. The black lines show the locations of the profiles in Fig. 2.

depth. Using a Clapeyron slope of 2.9 MPa K^{-1} for the 410 km discontinuity and –2.1 MPa K^{-1} for the 660 km discontinuity (Bina & Helffrich 1994), a thermal anomaly of >280 K would perturb the TZT by 30 km or more. Our result, showing an average TZT of 251 ± 10 km, therefore, demonstrates that a thermal anomaly of ≥280 K under the CVL does not likely extend as deep as the transition zone.

Reusch *et al.* (2010) argued that the model for the origin of the CVL most consistent with their tomographic images and the lack of an age progression in the volcanism in the CVL is the edge-flow model (King & Anderson 1998; King & Ritsema 2000; King 2007). The edge-flow model invokes a thermal downwelling adjacent to the colder Congo Craton lithosphere with a warm upwelling 200–700 km away, driven by the temperature difference between the thicker and cold Archean craton lithosphere and the adjacent convecting mantle under the thinner Proterozoic lithosphere. Because there is no observed thinning of the TZT nor any significant topography on the 410, this suggests that the convection cell is limited, perhaps by the magnitude of the thermal perturbation (King & Anderson 1998), to the upper ∼400 km of the mantle.

Thus, the results of this study are consistent with the edge flow model, strengthening its viability as a candidate model for the origin of the CVL. To illustrate further this finding, Fig. 4 shows the LVA under the CVL together with a sketch of the edge-flow convection pattern and the receiver functions stacks showing the P_s conversions from the 410 and 660 km discontinuities. The LVA in the tomographic image shown in this figure extends into the transition zone, but as explained by Reusch *et al.* (2010), there is more than 100 km of vertical smearing in the tomographic images, and thus the bottom of the LVA is probably at a depth of around 300 km, or perhaps even shallower.

The other model mentioned in the introduction that would be consistent with a slab-like LVA in the mantle under the CVL is the model from Meyers *et al.* (1998), in which shear heating from below the 660 km discontinuity gives rise to a vertical upwelling of hot material. The upwelling in this model comes from the base of the transition zone, and would be manifest as a thermal anomaly beginning at around 660 km depth. Such a deep-seated thermal anomaly is not consistent with the TZT beneath Cameroon, and therefore, this model is not favoured.

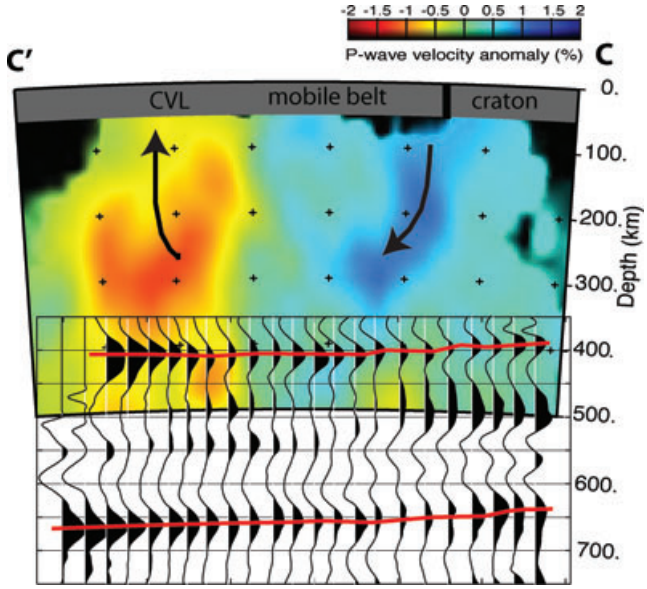

Figure 4. Cross-section along profile C–C′ (Fig. 3) showing the *P* wave tomographic image from Reusch *et al.* (2010) and the receiver-function stacks. The curves with arrows illustrate the model of edge-flow convection pattern along the northern edge of the cold Congo Craton lithosphere. The red lines mark the picks for the 410 and 660 km discontinuities, where evident.

ACKNOWLEDGMENTS

We would like to thank Garrett Euler, Alain-Pierre Tokam, Mike Fort and many other individuals for assistance in preparing, deploying and retrieving seismic stations and data, and Scott King and an anonymous reviewer for constructive reviews. This work was funded by the National Science Foundation under grants EAR 0310272, EAR 0310094 and OISE 0530062. The instruments used in the field program were provided by the PASSCAL facility of the Incorporated Research Institutions for Seismology (IRIS) through the PASSCAL Instrument Center at New Mexico Tech. Data collected during this experiment are available through the IRIS Data Management Center. The facilities of the IRIS Consortium are supported by the National Science Foundation under Cooperative Agreement EAR-0552316 and by the Department of Energy National Nuclear Security Administration.

REFERENCES

Bina, C.R. & Helffrich, G., 1994. Phase-transition Clapeyron slopes and transition zone seismic discontinuity topography, *J. geophys. Res.,* **99,** 15 853–15 860.

Burke, K., 2001. Origin of the Cameroon line of volcano-capped swells, *J. Geol.,* **109,** 349–362.

Chevrot, S., Vinnik, L. & Montagner, J.-P., 1999. Global-scale analysis of the mantle *Pds* phases, *J. geophys. Res.,* **104,** 20 203–20 219.

Courtier, A.M *et al*., 2007. Correlation of seismic and petrologic thermometers suggest deep thermal anomalies beneath hotspots, *Earth planet. Sci. Lett.,* **264,** 308–316.

Déruelle, B., Moreau, C., Nkoumbou, C., Kambou, R., Lissom, J., Njonfang, E., Ghogomu, R.T. & Nono, A., 1991. The Cameroon Line: a review, in *Magmatism in Extensional Tectonic Structural Settings,* pp. 274–327, eds Kampunzu, A.B. & Lubala, R.T., Springer, Berlin.

Ebinger, C.J. & Sleep, N.H., 1998. Cenozoic magmatism throughout east Africa resulting from impact of a single plume, *Nature,* **395,** 788–791.

Fairhead, J.D., 1988. Mesozoic plate tectonic reconstructions of the Central South-Atlantic Ocean – the role of the West and Central African rift system, *Tectonophysics,* **155,** 181–191.

Fairhead, J.D. & Binks, R.M., 1991. Differential opening of the Central and South-Atlantic oceans and the opening of the West African rift system, *Tectonophysics,* **187,** 191–203.

Fitton, J.G. & Dunlop, H.M., 1985, The Cameroon Line, West-Africa, and its bearing on the origin of oceanic and continental alkali basalt, *Earth planet. Sci. Lett.,* **72,** 23–38.

Flanagan, M.P. & Shearer, P.M., 1998. Global mapping of topography on transition zone velocity discontinuities by stacking SS precursors, *J. geophys. Res.,* **103,** 2673–2692.

Kennett, B.L.N. & Engdahl, E.R., 1991. Traveltimes for global earthquake location and phase identification, *Geophys. J. Int.,* **105,** 429–465.

King, S.D., 2007. Hotspots and edge-driven convection, *Geology,* **35,** 223–226.

King, S.D. & Anderson, D.L., 1995. An alternative mechanism of flood basalt formation, *Earth planet. Sci. Lett.,* **136,** 269–279.

King, S.D. & Anderson, D.L., 1998. Edge-driven convection, *Earth planet. Sci. Lett.,* **160,** 289–296.

King, S.D. & Ritsema, J., 2000. African hot spot volcanism: small-scale convection in the upper mantle beneath cratons, *Science,* **290,** 1137–1140.

Lawrence, J.F. & Shearer, P.M., 2006. A global study of transition zone thickness using receiver functions, *J. geophys. Res.,* **111,** B06307, doi:10.1029/2005JB003973.

Lee, D.-C., Halliday, A.N., Fitton, J.G. & Poli, G., 1994. Isotopic variations with distance and time in the volcanic islands of the Cameroon Line – evidence for a mantle plume origin, *Earth planet. Sci. Lett.,* **123,** 119–138.

Ligorría, J.P. & Ammon, C.J., 1999. Iterative deconvolution and receiver-function estimation, *Bull. seism. Soc. Am.,* **89,** 1395–1400.

Marzoli, A., Renne, P.R., Piccirillo, E.M., Francesca, C., Bellieni, G., Melfi, A.J. Nyobe, J.B. & N'ni, J., 1999. Silicic magmas from the continental Cameroon Volcanic Line (Oku, Bambouto and Ngaoundere): Ar-40-Ar-39 dates, petrology, Sr-Nd-O isotopes and their petrogenetic significance, *Contrib. Mineral. Petrol.,* **135,** 133–150.

Marzoli, A., Piccirillo, E.M., Renne, P.R., Bellieni, G., Iacumin, M., Nyobe, J.B. & Tongwa, A.T., 2000. The Cameroon Volcanic Line revisited: petrogenesis of continental basaltic magmas from lithospheric and asthenospheric mantle sources, *J. Petrol.,* **41,** 87–109.

Meyers, J.B., Rosendahl, B.R., Harrison, C.G.A., & Ding, Z.-D., 1998. Deep-imaging seismic and gravity results from the offshore Cameroon volcanic line, and speculation of African hotlines, *Tectonophysics,* **284,** 31–63.

Morgan, W.J., 1983, Hotspot tracks and the early rifting of the Atlantic, *Tectonophysics,* **94,** 123–139.

Ngako, V., Njonfang, E., Aka, F.T., Affaton, P. & Nnange, J.M., 2006. The North–South Paleozoic to Quaternary trend of alkaline magmatism from Niger–Nigeria to Cameroon: complex interaction between hotspots and Precambrian faults, *J. Afr. Earth Sci.,* **45,** 241–256.

Owens, T.J., Nyblade, A.A., Gurrola, H. & Langston, C.A., 2000. Mantle transition zone structure beneath Tanzania, East Africa, *Geophys. Res. Lett.,* **27,** 827–830.

Reusch, A.M., Nyblade, A.A., Wiens, D.A., Shore, P.J., Ateba, B., Tabod, C.T. & Nnange, J.M., 2010. Upper mantle structure beneath Cameroon from body wave tomography and the origin of the Cameroon Volcanic Line, *Geochem. Geophys. Geosyst.,* **11,** Q10W07, doi:10.1029/2010GC003200.

Tibi, R., Larson, A.M., Nyblade, A.A., Shore, P.J., Wiens, D.A., Nnange, J.M., Tabod, C. & Bekoa, A., 2005. A broadband seismological investigation of the Cameroon Volcanic Line. *EOS, Trans. Am. geophys. Un.,* **86**(52), Fall Meet. Suppl., Abstract S11B-0170.

Tokam, A.P., Tabod, C.T., Nyblade, A., Julia, J., Wiens, D.A. & Pasyanos, M.E., 2010. Structure of the crust beneath Cameroon, West Africa, from the joint inversion of Rayleigh wave group velocities and receiver functions, *Geophys. J. Int.,* **183,** 1061–1076, doi:10.1111/j.1365-246.2010.04776.

Van Houten, F.B., 1983. Sirte Basin, north-central Libya: cretaceous rifting above a fixed mantle hotspot, *Geology,* **11,** 115–118.